

Infrared Spectroscopy and X-Ray Diffraction Studies of C–H...O Hydrogen Bonding and Thermal Behavior of Biodegradable Poly(hydroxyalkanoate)

Harumi Sato,*¹ Rumi Murakami,¹ Jianming Zhang,¹ Katsuhito Mori,¹
Isao Takahashi,¹ Hikaru Terauchi,¹ Isao Noda,² Yukihiro Ozaki¹

Summary: Infrared (IR) spectra and wide-angle X-ray diffraction (WAXD) patterns of poly(3-hydroxybutyrate) (PHB) and its copolyester, poly(3-hydroxybutyrate-co-3-hydroxyhexanoate), P(HB-co-HHx) (HHx = 12 mol%) were measured over a temperature range of 20 °C to higher temperatures (PHB, 185 °C, HHx = 12 mol%, 140 °C) to explore their structure change and thermal behavior and molecular interaction. The WAXD measurements revealed that the *a* lattice parameter increases significantly with temperature, while the *b* lattice parameter varies a little in the crystalline PHB and P(HB-co-HHx). It seems that the intermolecular interaction between the C=O group of one helical structure and the CH₃ group of the other helical structure decreases along the *a* axis of crystalline PHB and P(HB-co-HHx) with temperature. The temperature-dependent IR spectral variations were analyzed for the CH stretching, C=O stretching, CH₃ deformation, and C–O–C stretching variation regions, and bands characteristic of crystalline and amorphous parts were identified in each region. It was found from the anomalous frequencies of the CH₃ asymmetric stretching and C=O stretching bands of PHB and P(HB-co-HHx) and the X-ray crystallographic structure of PHB that there is an intermolecular interaction (C–H...O=C hydrogen bond) between the C=O group and the CH₃ group combining two helical structures in PHB and P(HB-co-HHx). In this review paper we discuss the role of the C–H...O=C hydrogen bonding and the crystal and lamella structure of PHB and P(HB-co-HHx) (HHx = 12 mol %) in comparison with the structure of Nylon.

Keywords: biodegradable polymers; C–H...O hydrogen bonding; crystallinity; infrared spectroscopy; poly(hydroxyalkanoate); thermal behavior; X-ray diffraction

Introduction

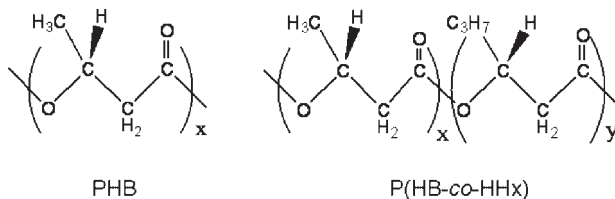
Poly(3-hydroxybutyrate) (PHB) (Figure 1) is an optically active aliphatic polyester with a relatively low glass transition temperature (around 5 °C) produced by bacterial fermentation.^[1–10] PHB is biodegradable and its physical properties are fairly similar to those of certain petroleum-based synthetic polymers. For example, the

mechanical property of PHB is similar to that of isotactic polypropylene. However, because of the high stereoregularity of biologically produced macromolecules, it is highly crystalline and, hence, too rigid, stiff, and brittle. To reduce the crystallinity and increase the flexibility of PHB, a longer side-chain 3-hydroxyhexanoate (3-HHx) comonomer is copolymerized with 3-hydroxybutyrate (3-HB) units.^[10–13] The resulting P(HB-co-HHx) copolymers possess dramatically improved physical and mechanical properties compared with those of PHB homopolymer.

The structures, thermal behavior, and mechanical properties of PHB and

¹ School of Science and Technology, and Research Center for Environment Friendly Polymers, Kwansei-Gakuin University, Sanda 669-1337, Japan

² The Procter and Gamble Company, 8611 Beckett Road, West Chester, Ohio 45069, USA

**Figure 1.**

Chemical structures of poly(3-hydroxybutyrate) (PHB) and poly(3-hydroxybutyrate-co-3-hydroxyhexanoate) (P(HB-co-HHx)).

P(HB-co-HHx) were investigated by several research groups.^[10–13] It has been found from X-ray crystallographic studies that PHB crystallizes into a 2₁-helix with an approximately g^+g^{+t} conformation, and the crystal structure of isolated PHB consists of an orthorhombic unit cell that contains two left-handed helical molecules in antiparallel orientation.^[14,15] The single crystal of PHB shows a peculiar formation of folded chain in the lamellae structure.^[16] Based on the molecular weight studies on depolymerase-treated single crystals of PHB, Marchessault et al.^[17] suggested that the PHB single crystals create a multiple erosion surface in the fold plane direction, i.e. parallel to the long axis (*a* axis of unit cell). They suggested that the antiparallel chain packing of PHB which provides a relatively stable tubular ribbon in the first stage of chain folding encourages subsequent selfassembly of precursor elements.

The lamellar thickness of PHB homopolymer and its copolymers was investigated by Abe et al.^[18] by using Small-angle X-ray scattering (SAXS). It was found that the lamellar thickness of P(HB-co-HHx) with the high HHx content (e.g. 1.9 nm for HHx = 8 mol%) is much thinner than that of PHB (5.3 nm). The second monomer units of P(HB-co-HHx) are excluded from the PHB crystalline regions and they may exist mainly on the crystal surface. This is the reason why the lattice spacing of P(HB-co-HHx) is essentially the same as that of PHB.

We have been investigating the molecular and crystalline structures of PHB and P(HB-co-HHx) by means of Wide-angle X-ray diffraction (WAXD), infrared (IR)

spectroscopy, and differential scanning calorimetry (DSC).^[20–25] Particular attention has been paid to the interaction between the C=O and CH₃ groups of PHB and P(HB-co-HHx). The temperature-dependent WAXD study suggested that there is a peculiar intermolecular interaction between the C=O and CH₃ groups along the *a* axis of the crystal lattice, and the interaction decreases with temperature.^[20] Subsequently, the existence and thermally induced changes of the C–H...O=C hydrogen bond between the C=O group in one helical structure and the CH₃ group in the other helical structure were verified by a temperature-dependent IR spectroscopy study of PHB and P(HB-co-HHx).^[21] It is very likely that a chain of C–H...O=C hydrogen bond pairs link two parallel helical structures in the crystalline parts.^[21] The temperature-dependent IR spectral variations revealed that the crystallinity of P(HB-co-HHx) (HHx = 12 mol%) decreases gradually from a fairly low temperature (about 60 °C), while the crystallinity of PHB remains almost unchanged until just below its melting temperature.^[21] It was also found from the IR studies that for both PHB and P(HB-co-HHx) the weakening of the C–H...O=C hydrogen bonds starts from just above room temperature.

This review paper reports the results of our recent WAXD and IR studies on the C–H...O=C hydrogen bond^[26–29] and thermal behavior of PHB and P(HB-co-HHx) and discuss the role of the C–H...O=C hydrogen bondings and the crystal and lamella structure of PHB and P(HB-co-HHx) (HHx = 12 mol%) in comparison with the structure of Nylon.

Experimental

Samples

Bacterially synthesized PHB and P(HB-*co*-HHx) (HHx = 12 mol%) were obtained from the Procter & Gamble Company, Cincinnati, OH. They were dissolved in hot chloroform, re-precipitated in methanol as fine powder, and vacuum-dried at 60 °C. The purified P(HB-*co*-HHx) sample thus obtained was used in all experiments.

Wide-angle X-ray Diffraction (WAXD)

The WAXD data were measured for the precipitated powder samples of PHB and P(HB-*co*-HHx) over a temperature range from 30.1 to 165 °C (PHB) or to 105.8 °C (P(HB-*co*-HHx)) in the scattering angle range of $2\theta = 5\text{--}13^\circ$ by using a two-circle Rigaku X-ray diffractometer equipped with a scintillation detector. Radiation of wavelength 0.71069 Å (Mo-K α) was employed at generator power of 40 kV and 240 mA. The temperature dependence of the WAXD measurement was controlled by a thermoelectric device (CN4400, OMEGA) with an accuracy of $\pm 0.1^\circ\text{C}$. The heating rate was ca. 1 °C/min. The calibration of the WAXD patterns was carried out by the method reported in reference 20.

IR Measurements

Films of PHB and P(HB-*co*-HHx) were prepared by casting their chloroform solutions on CaF₂ windows. The films were kept in a vacuum-dried oven at 60 °C for 12 hours, and cooled down to room temperature. The transmission IR spectra were measured at a 2 cm⁻¹ resolution using a Thermo Nicolet NEXUS 470 Fourier transform IR spectrometer with a liquid-nitrogen-cooled mercury-cadmium-telluride detector. A total of 512 scans were co-added for each IR spectral measurement to ensure a high signal-to-noise ratio. The temperature of the IR cell was controlled by a thermoelectric device (CN4400, OMEGA) with an accuracy of $\pm 0.1^\circ\text{C}$. The temperature was increased at a rate of ca. 2 °C/min. After changing the temperature, the cell was maintained at that temper-

ature for 15 min to make the samples equilibrate.

Results and Discussion

Wide-Angle X-Ray Diffraction (WAXD)

Studies of PHB and P(HB-*co*-HHx)

The WAXD measurements were carried out for PHB and P(HB-*co*-HHx) (HHx = 12 mol%) over a temperature range from 25 to 165 °C (PHB) or to 140 °C P(HB-*co*-HHx) (HHx = 12 mol %).^[20] The melting points of PHB and P(HB-*co*-HHx) (HHx = 12 mol%) revealed by DSC are 170 and 106 °C, respectively. It was found from the WAXD measurements that the (110) d-spacing of PHB and P(HB-*co*-HHx) lattice expands as temperature increases while their (020) d-spacing changes little. These results mean that the *a* lattice parameter increases significantly while the *b* lattice parameter varies little as a function of temperature.^[20] Figure 2a plots $\Delta a/a_0$ and $\Delta b/b_0$ versus temperature. Here, *a*₀ and *b*₀ are lattice parameters at 25 °C and Δa (or Δb) is a difference between *a*₀ (or *b*₀) at 25 °C and the lattice parameter, *a* (or *b*) at the temperature measured.^[25] It has to be noted that $\Delta a/a_0$ increases linearly from room temperature while $\Delta b/b_0$ changes little. Similar results were obtained also for P(HB-*co*-HHx) (HHx = 2.5, 3.5, and 10.5 mol %).^[25] The thermal expansion in the *a* axis indicated that there is an interchain interaction between the C=O group of one helical structure and the CH₃ group of the other helical structure because they are closely located to each other along the *a* axis. Quite recently, we explored the reversibility of the variations in the *a* and *b* lattice parameters for PHB and P(HB-*co*-HHx) and found that the values of the *a* lattice parameters at room temperature before the heating process and after the cooling process are almost the same, while the corresponding values of the *b* lattice parameters are significantly different.^[25] In other words, the *a* lattice parameters vary reversibly. This also suggested that there is an interchain interaction along the *a* axis.

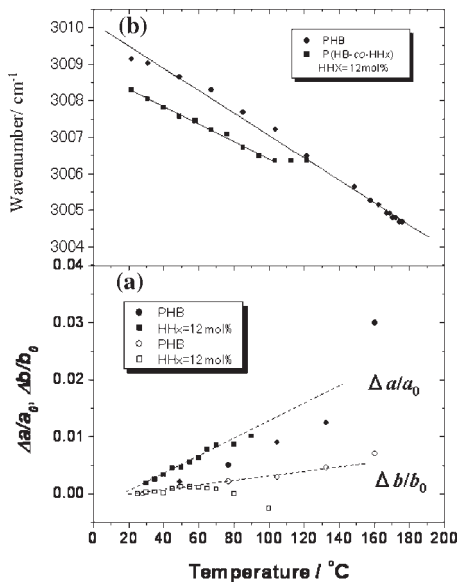


Figure 2.

a) Temperature-dependent variations of $\Delta a/a_0$ and $\Delta b/b_0$. a_0 and b_0 are lattice parameters at 25 °C and Δa (or Δb) is a difference between a_0 (or b_0) and the lattice parameter, a (or b), at a particular temperature. b) Temperature-dependent variations of the wavenumber of the CH stretching band at 3009 cm⁻¹ for PHB and P(HB-co-HHx) (HHx = 12 mol %).

In Figure 3a, the temperature dependences of the normalized peak area of the (110) reflection are compared for PHB and P(HB-co-HHx) (HHx = 12 mol %). The peak area of the P(HB-co-HHx) copolymer shows a gradual change with temperature from a fairly low temperature (60 °C), while that of PHB changes little until a fairly high temperature and decreases suddenly near its melting temperature (160 °C).^[20] These results suggested that the thermal behavior is quite different between PHB and P(HB-co-HHx) (HHx = 12 mol %). The WAXD results shown in Figure 3a revealed that the crystallinity of PHB remains high until just below its melting temperature while that of P(HB-co-HHx) (HHx = 12 mol %) decreases gradually from a fairly low temperature (60 °C).^[20] It is very likely that the addition of HHx groups affects significantly the thermal behavior of PHA.

Figures 4a and b show IR spectra in the 3050–2800 cm⁻¹ region of PHB and P(HB-

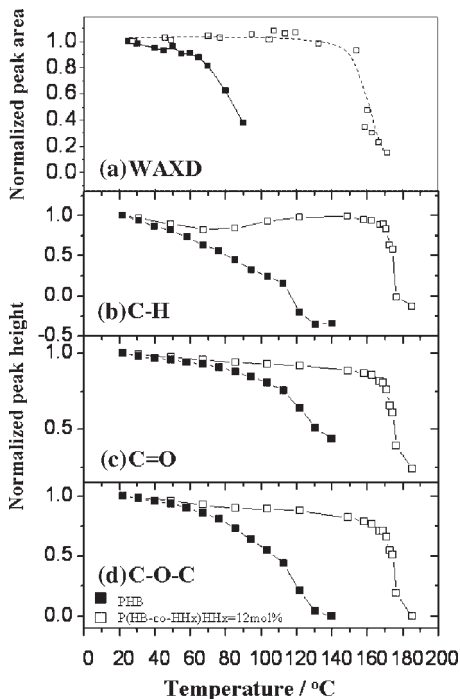


Figure 3.

a) Temperature dependences of the normalized peak area of the (110) reflection for PHB and P(HB-co-HHx) (HHx = 12 mol %). b) Temperature-dependent variations of the peak height of the CH stretching band at 3009 cm⁻¹ in the second derivative spectra of PHB and P(HB-co-HHx) (HHx = 12 mol %). c) and d) Temperature-dependent variations of the peak heights of the C=O stretching band at 1723 cm⁻¹ and the C-O-C stretching band at 1228 cm⁻¹ in the spectra of PHB and P(HB-co-HHx) (HHx = 12 mol %).

co-HHx) (HHx = 12 mol %) collected over a temperature range of 21 °C to a high temperature (PHB; 185 °C, HHx = 12 mol %, 140 °C).^[21] Their second derivatives are displayed in Figures 5a and b, respectively.^[21] Note that the calculation of the second derivative spectra is powerful in dissolving the overlapping bands in the 3050–2800 cm⁻¹ region. The band assignments in this spectral region are still not clear, but five bands at 3009, 2995, 2983, 2974, and 2967 cm⁻¹ may be assigned to the CH₃ asymmetric stretching modes.^[21] Only the band at 2983 cm⁻¹ increases with temperature, and thus it arises from the amorphous parts. The other bands at 3009, 2995, 2974, and 2967 cm⁻¹ are ascribed to

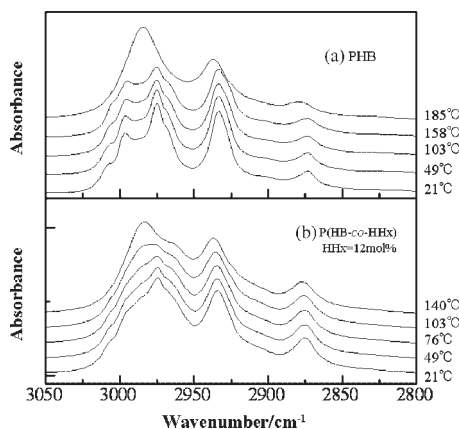


Figure 4. IR spectra in the 3050–2800 cm^{-1} region of PHB and P(HB-co-HHx) (HHx = 12 mol%) measured over a temperature range of 21 °C to a high temperature (PHB; 185 °C, P(HB-co-HHx) (HHx = 12 mol%); 140 °C).

the crystalline parts. The most important finding in the 3050–2800 cm^{-1} region was that one CH_3 asymmetric stretching band appears at an unusually high frequency (3009 cm^{-1}).^[21] This frequency is higher by ca. 25 cm^{-1} than that of the CH_3 asymmetric stretching band of the amorphous parts. Poly(L-lactide) (PLLA) shows a CH_3 asymmetric stretching band at 2989 cm^{-1} .^[30] Therefore, these observations, together with the results of quantum chemical calculation led us to conclude that the

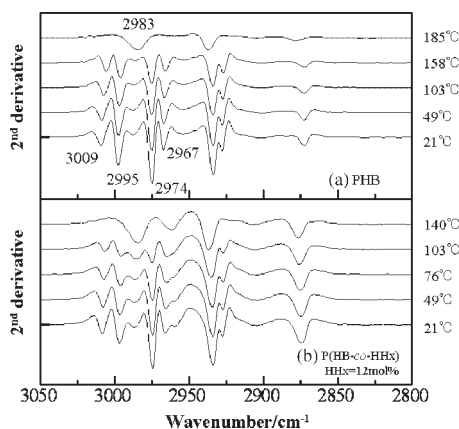


Figure 5. The second derivatives of the spectra shown in Figure 4.

3009 cm^{-1} band is due to the C–H stretching (pseudo CH_3 asymmetric stretching) mode of the C–H...O=C hydrogen bonding.^[21,22] One must notice that the frequency of the CH stretching band near 3009 cm^{-1} is slightly lower for P(HB-co-HHx) (HHx = 12 mol %) (3008 cm^{-1}) than for PHB (3010 cm^{-1}).^[25] The difference is very small but reproducible. This result indicated that the C–H...O=C hydrogen bonding is slightly weaker in P(HB-co-HHx) than in PHB.^[25] Some support for this conclusion comes from the fact that the *a* lattice parameter is slightly larger in P(HB-co-HHx) (HHx = 12 mol%) than in PHB.^[25]

It has to be noted in Figure 2b and 3b that the CH-stretching bands at 3009 cm^{-1} of both PHB and P(HB-co-HHx) show a linear low frequency shift as temperature increases and that the intensity of the 3009 cm^{-1} band of PHB changes a little until just below the melting temperature but that of P(HB-co-HHx) decreases gradually from a fairly low temperature.^[21,25] It seems very likely that the C–H...O=C hydrogen bonding becomes weak gradually from room temperature in both PHB and P(HB-co-HHx) and that the bonding is more easily broken in P(HB-co-HHx) than in PHB.^[25] It is also interesting to note that the temperature-dependent variations in the wavenumber range of the CH stretching band are in parallel with those of the *a* lattice parameter (Figure 2). Thus, as the *a* lattice parameter increases, the hydrogen bonding becomes weak.

Figures 6a and b show IR spectra in the 1800–1150 cm^{-1} region of films of PHB and P(HB-co-HHx) (HHx = 12 mol %) measured over a temperature range of 21 °C to a high temperature (PHB; 185 °C, P(HB-co-HHx); 140 °C). The C=O stretching band region consists of two major bands; one sharp band at 1723 cm^{-1} and one broad band centered at 1740 cm^{-1} .^[21] The former is intense at room temperature, but its intensity decreases as temperature increases while the intensity of the latter increases with temperature. At the highest temperature only the broad band near

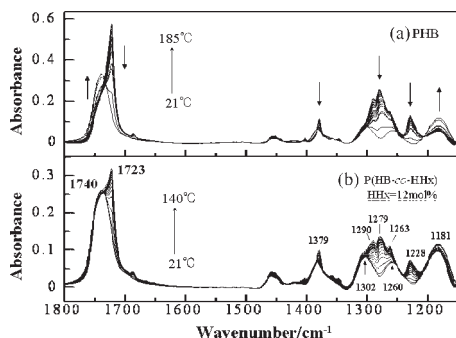


Figure 6.

IR spectra in the 1800–1150 cm^{-1} region of films of (a) PHB and (b) P(HB-co-HHx) (HHx = 12 mol %) measured over a temperature range of 21 °C to a high temperature (PHB; 185 °C, P(HB-co-HHx) (HHx = 12 mol %); 140 °C).

1740 cm^{-1} remains in the C=O stretching region. Therefore, the sharp band at 1723 cm^{-1} and the broad band at 1740 cm^{-1} are assigned to the C=O stretching modes of the crystalline and amorphous parts, respectively.^[21] It has to be noted that the relative intensity of the 1740 cm^{-1} band is much stronger in the spectrum of P(HB-co-HHx) than in that of PHB at room temperature. This observation is in good agreement with the fact that the crystallinity of PHB (60 %) is much higher than that of P(HB-co-HHx) (35 %).

Of particular note in Figure 6 is that the crystalline C=O stretching bands of PHB and P(HB-co-HHx) appear at an unusually low frequency (1723 cm^{-1}) compared with those of polyesters.^[21,22] For example, PLLA shows a crystalline C=O stretching band at 1761 cm^{-1} .^[30] Thus, the positions of the amorphous C=O bands of PHB and P(HB-co-HHx) are normal but those of the crystalline C=O bands are much lower than usual. Based on the quantum chemical calculation of the low-frequency shift of the C=O band for the dimer of a model compound of PHB, $\text{CH}_3\text{CH}(\text{CH}_3)\text{O}-\text{COCH}_2\text{CH}_3$, at the B3LYP/cc-pVDZ level, we concluded that the large low-frequency shift of the crystalline C=O stretching band arises from the formation of C–H...O=C hydrogen bonding.^[22] In Figure 3c the normalized peak height of the C=O

stretching band at 1723 cm^{-1} of PHB and P(HB-co-HHx) (HHx = 12 mol %) due to the crystalline state is plotted as a function of temperature.^[21] It is found from Figures 3b and c that the temperature-dependent intensity changes of the crystalline C=O stretching bands of PHB and P(HB-co-HHx) proceed in parallel with those of the crystalline CH stretching bands of the CH_3 group. This confirms that the temperature-dependent variations of both C=O and CH stretching bands reflect thermal behavior of the C–H...O=C hydrogen bonding.

In the 1400–1350 cm^{-1} region a band at 1378 cm^{-1} is assigned to the symmetric deformation mode of the CH_3 group.^[22] It is well known that the frequency of a CH_3 symmetric deformation band is sensitive to the conformation of a helical structure of a polymer. The frequency of the 1378 cm^{-1} band of PHB changes little until just below the melting temperature while that of P(HB-co-HHx) (HHx = 12 mol %) varies gradually from a fairly low temperature. These results indicated that the helical structure of PHB is fairly stable against temperature but that of the copolymer deforms gradually from the fairly low temperature.^[22]

The spectra in the 1320–1150 cm^{-1} region contain not only bands due to the C–O–C stretching modes but also those due to the CH and CH_2 bending modes. It is noted that five bands at 1289, 1279, 1263, 1228, and 1182 cm^{-1} dominate the spectra at room temperature, while the spectra at high temperatures consist of three major features near 1302, 1257, and 1180 cm^{-1} .^[21] The four bands at 1289, 1279, 1263, and 1228 cm^{-1} do not appear in the spectra measured at high temperatures whereas those at 1302 and 1257 cm^{-1} appear only weakly as a shoulder in the spectra at room temperature. Accordingly, we assigned bands at 1289, 1279, 1263, and 1228 cm^{-1} to the crystalline state and attributed those at 1302 and 1257 cm^{-1} to the amorphous state.^[21] It is well known that the bands in this region are very sensitive to the conformation of a polymer. The four bands at 1289, 1279, 1263, and 1228 cm^{-1} reflect the helical structure whereas the two bands

at 1302 and 1228 cm^{-1} arise from the random structures.

It has to be noted that the frequencies of the four crystalline bands are almost identical between the two kinds of PHAs, suggesting that the helical structures of the crystalline states of the two PHAs are very similar to each other.^[21] Therefore, the structural differences between PHB and P(HB-*co*-HHx) (HHx = 12 mol%) do not lie in the structures of the crystalline states themselves but lie in the ratio between the crystalline and amorphous components. In other words, the inclusion of the HHx comonomers does not modify the helical

structure but cut down the helical structures from place to place, leading to the reduction of crystallinity.

Figure 3d plots the normalized peak height of the band near 1228 cm^{-1} due to the crystalline state versus temperature for PHB and P(HB-*co*-HHx) (HHx = 12 mol%). Interesting enough, the temperature-dependent variations in the bands at 3009 and 1723 cm^{-1} are very similar to those in the band at 1228 cm^{-1} (Figures 3b, c, and d). Therefore, the cleavage of the C-H...O=C hydrogen bondings proceeds in parallel with the helical structure change.

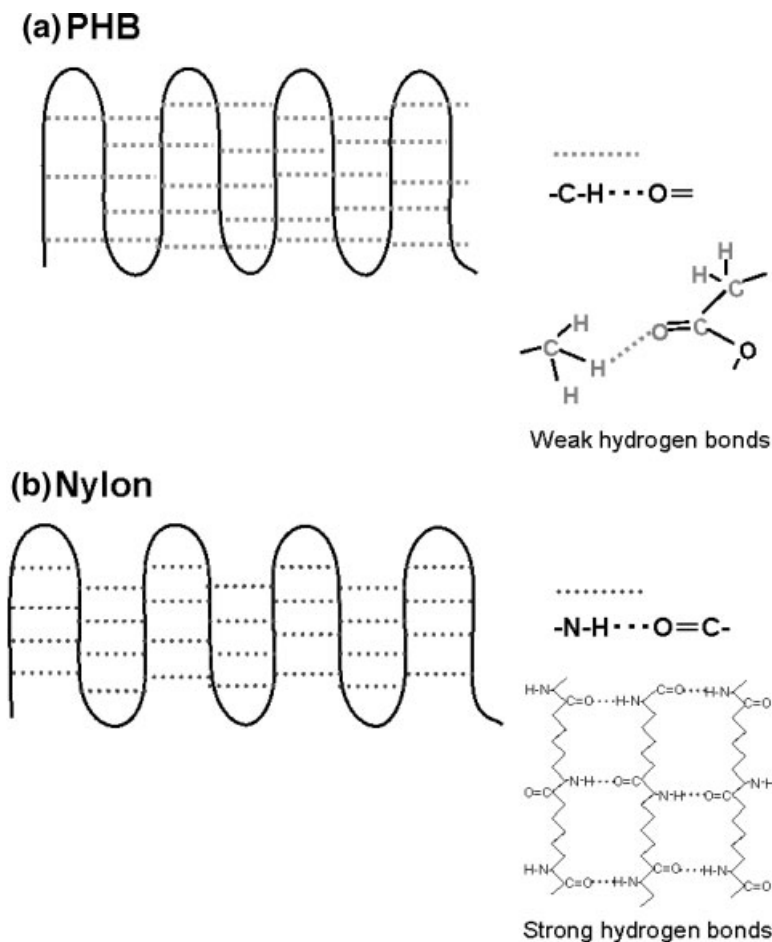


Figure 7.

a) C-H...O=C hydrogen bonding network in PHB and b) N-H...O=C hydrogen bonding network in Nylon.

Comparison of Hydrogen Bonding Network in PHB and P(HB-co-HHx) (HHx = 12 mol%) with that in Nylon

It is of particular interest to compare the C–H...O=C hydrogen bonding network in PHB and P(HB-co-HHx) (HHx = 12 mol %) with the N–H...O=C hydrogen bonding network in Nylon. Figure 7 illustrates structural models for the hydrogen bonding networks of a) PHB and b) Nylon. It is well known that in Nylon strong N–H...O=C hydrogen bondings play a very important role in stabilizing the lamella structure.^[31] The hydrogen bondings combine two antiparallel helical chains. The hydrogen network of Nylon develops along the *b* axis, and the *b* lattice parameter changes a little until just below the melting temperature probably because the N–H...O=C hydrogen bonding is thermally stable. The hydrogen bondings are not broken until just below the melting temperature, and the *a* axis increases more significantly than the *b* axis with temperature below the melting temperature in Nylon. As in the case of Nylon, the *a* axis increases more significantly than the *b* axis with temperature for PHB. However, the situation is quite different for PHB because the C–H...O=C hydrogen bonding is much weaker than the N–H...O=C hydrogen bonding (the bonding energy of the C–H...O=C hydrogen bond in the dimer of CH₃CH(CH₃)OCOCH₂CH₃ was calculated to be 1.22 kcal/mol^[31] while that of the N–H...O=C bond in Nylon was reported to be 4.321 kcal/mol/amide unit^[32]). Thus, the C–H...O=C hydrogen bond becomes weak even just above room temperature, leading to the increase in the *a* lattice parameter. Our recent study^[25] suggested that the formation of C–H...O=C hydrogen bonding between two antiparallel helical chains stabilizes the lamella structure of PHB and P(HB-co-HHx) and that the high crystallinity of PHB and P(HB-co-HHx) partly comes from the C–H...O=C hydrogen bonding.

Acknowledgements: The authors thank Prof. Koji Tashiro (Toyota Technological Institute)

and Prof. Tadahisa Iwata (RIKEN) for valuable discussion. This work was partially supported by “Open Research Center” project for private universities: matching fund subsidy from MEXT (Ministry of Education, Culture, Sports, Science and Technology), 2001–2005. This work was supported also by Kwansei-Gakuin University “Special Research” project, 2004–2008.

- [1] M. Lemoigne, *Bull. Soc. Chim. Biol.* **1926**, 8, 770.
- [2] Y. Doi, *Microbial Polyesters*, VCH Publishers, New York (1990).
- [3] A. J. Anderson and E. A. Dawes, *Microbiol. Rev.*, **1990**, 54, 450.
- [4] E. Chiellini, and R. Solaro, “Recent Advances in Biodegradable Polymers and Plastics”, Wiley-VCH, Weinheim, 2003.
- [5] Y. Doi, “ICBP 2003 First IUPAC International Conference on Bio-Based Polymers, Macromolecular Bioscience”, Vol. 4, Issue 3, WILEY-VCH, Weinheim, 2004.
- [6] C. Bastioli, “Handbook of Biodegradable Polymers”, Rapra Technology Limited, 2005.
- [7] M. Vert, *Biomacromolecules* **2005**, 6, 538.
- [8] M. M. Satkowski, D. H. Melik, J. P. Autran, P. R. Green, I. Noda, and L. A. Schechtman, “Biopolymers”, Steinbüchel, A, Y. Doi Eds., Wiley-VCH, Weinheim, 2001, p231.
- [9] Y. Doi, S. Kitamura, and H. Abe, *Macromolecules* **1995**, 28, 4822.
- [10] G. Kobayashi, T. Shiotani, Y. Shima, and Y. Doi, “In Biodegradable Plastics and Polymers”, Y. Doi and K. Fukuda Eds. Elsevier, Amsterdam, 1994, p410.
- [11] Web site: www.nodax.com.
- [12] M. Kunioka, A. Tamaki, and Y. Doi, *Macromolecules* **1989**, 22, 694.
- [13] N. Yoshie, H. Menju, H. Sato, and Y. Inoue, *Macromolecules* **1995**, 28, 6516.
- [14] J. Cornibert, R. H. Marchessault, *J. Mol. Biol.* **1972**, 71, 735.
- [15] M. Yokouchi, Y. Chatani, H. Tadokoro, K. Teranishi, and H. Tani, *Polymer* **1973**, 14, 267.
- [16] F. Su, T. Iwata, K. Sudesh, Y. Doi, *Polymer* **2001**, 42, 8915.
- [17] R. H. Marchessault and J. Kawada, *Macromolecules* **2004**, 37, 7418.
- [18] H. Abe, Y. Doi, H. Aoki, and T. Akehata, *Macromolecules* **1998**, 31, 1791.
- [19] T. Iwata, M. Shiromo, and Y. Doi, *Macromol. Chem. Phys.* **2002**, 203, 1309.
- [20] H. Sato, M. Nakamura, A. Padermshoke, H. Yamaguchi, H. Terauchi, S. Ekgasit, I. Noda, and Y. Ozaki, *Macromolecules* **2004**, 37, 3763.
- [21] H. Sato, H. R. Murakami, A. Padermshoke, F. Hirose, K. Senda, I. Noda, and Y. Ozaki, *Macromolecules* **2004**, 37, 7203.
- [22] H. Sato, J. Dybal, R. Murakami, I. Noda, and Y. Ozaki, *J. Mol. Struct.* **2005**, 744–745, 35.

- [23] H. Sato, A. Padermshoke, M. Nakamura, R. Murakami, F. Hirose, K. Senda, H. Terauchi, S. Ekgasit, I. Noda, and Y. Ozaki, *Macromol. Symp.* **2005**, 220, 123.
- [24] A. Padermshoke, Y. Katsumoto, H. Sato, S. Ekgasit, I. Noda, and Y. Ozaki, *Polymer* **2004**, 45, 6547.
- [25] H. Sato, K. Mori, R. Murakami, Y. Ando, I. Takahashi, J. Zhang, H. Terauchi, F. Hirose, K. Senda, K. Tashiro, I. Noda, and Y. Ozaki, submitted for publication.
- [26] G. R. Desiraju and T. Steiner, *The Weak Hydrogen Bond — In Structural Chemistry and Biology*, Oxford University Press, 1999, p29–121.
- [27] H. Matsuura, H. Yoshida, M. Hieda, S. Yamanaka, T. Harada, K. Shin-ya, and K. Ohno, *J. Am. Chem. Soc.* **2003**, 125, 13910.
- [28] S. Scheiner and T. Kar, *J. Phys. Chem. A* **2002**, 106, 1784.
- [29] P. Hobza, Z. Havlas, *Chem. Rev.* **2000**, 100, 4253.
- [30] J. Zhang, H. Sato, I. Noda, and Y. Ozaki, *Macromolecules* **2005**, 38, 4274.
- [31] H. Sato, J. Dybal, T. Iwata, R. Murakami, J. Zhang, K. Tashiro, I. Noda, and Yukihiro Ozaki, submitted for publication.
- [32] Youyong Li and William A. GoddardIII, *Macromolecules* **2002**, 35, 8440.